Superionic behavior of lithium oxide Li_2O: A lattice dynamics and molecular dynamics study

Prabhatasree Goel, N. Choudhury, and S. L. Chaplot
Solid State Physics Division, Bhabha Atomic Research Centre, Trombay, Mumbai 400 085, India
(Received 18 June 2004; published 24 November 2004)

We report a cumulative study of lithium oxide in its normal as well as superionic phase using both lattice dynamical and molecular dynamical calculations. Molecular dynamics simulations have been carried out to study the fast ion phase and the diffusion behavior of lithium and oxygen ions. The results obtained for the diffusion constant and the thermal amplitude of lithium are in very good agreement with experimental observations. The pair correlation functions, Li—O—Li bond angle distribution and snapshots of the positions of lithium atoms over a range of time steps, provide a microscopic picture of the local structure indicating that as in other fluorites, the lithium ions diffuse via an interstitial mechanism but the distortions due to this movement are small. Lattice dynamical calculations have been done using a shell model in the quasiharmonic approximation. We have calculated the equilibrium structure, phonon frequencies, the elastic constants and the specific heat, which are in excellent agreement with the available experimental data. We also predict the pressure variation of the phonon dispersion and the equation of state.

DOI: 10.1103/PhysRevB.70.174307 PACS number(s): 66.30.Hs, 63.20.Dj, 65.40.−b

I. INTRODUCTION

Lithium oxide exhibits high ionic conductivity while in solid condition, and belongs to the class of superionics, which allow macroscopic movement of ions through their structure. This behavior is characterized by the rapid diffusion of a significant fraction of one of the constituent species within an essentially rigid framework formed by the other species. In lithium oxide, Li ion is the diffusing species, while oxygen ions constitute the rigid framework.[1,2] Lithium oxide, like other superionics, finds several technological applications. These applications range from miniature lightweight high power density lithium ion batteries for heart pacemakers, mobile phones, laptop computers, etc. to high capacity energy storage devices for next generation "clean" electric vehicles to name a few.[3] It is also a leading contender for future fusion reactors to convert energetic neutrons to usable heat and to breed tritium necessary to sustain *D-T* (deuterium-tritium) reaction.[3–5] This application is attributed to its high melting point, relatively low volatility and high Li atom density.

Microscopic modeling or simulation is necessary to understand the conduction processes at high temperatures in crystals. Several theoretical[6–15] and experimental[16–32] works have been reported on Li_2O,[6–13,25–32] CuI,[14,15] CaF_2, BaF_2, $SrCl_2$, PbF_2, etc.[16–24] The sole purpose of these studies has been to understand the process of fast ion conduction and the role of defects in conductivity; in case of Li_2O, further interest has been to study Li diffusion from the point of view of tritium generation for future fusion reactors.[5] Fluorites like CaF_2, BaF_2, $SrCl_2$, PbF_2, etc. show type II superionic transition.[3] They attain high levels of ionic conductivity following a gradual and continuous disordering process within the same phase. In general, this extensive diffusion is assumed to be associated with the development of extensive Frenkel disorder in the anion sublattice (cation in the case of antifluorites). This is characterized by a large decrease in the elastic constant C_{11}[20,22] and a specific heat anomaly[19–26] (a Schottky hump) at the transition temperature, T_c. The antifluorite lithium oxide is a face-centered-cubic structure belonging to the space group O^5_h ($Fm3m$). Lithium atoms are in tetrahedral sites. Similar to the other fluorites, this system too shows a sudden decrease in the value of the C_{11} elastic constant[27] at the transition temperature,[30] $T_c \sim 1200$ K (the melting point of Li_2O is 1705 K) although there does not seem to be any drastic change in the specific heat.[27–29] The diffusion coefficient of lithium at this transition becomes comparable to that of liquids.[30] Theoretical calculations have been done to formulate an interatomic potential for Li_2O[6,7] and several thermodynamic properties including lithium's diffusion coefficient, etc. have been calculated. Detailed study of the processes occurring in the crystal lattice at elevated temperatures is essential to understand the transition; to determine the probable interstitial regions where a given lithium atom resides while diffusing and to unravel the mystery as to why the local structure remains more or less maintained even beyond the transition temperature.

The main objectives of the present study are: (i) to formulate a suitable interatomic potential model to calculate the phonon spectrum, specific heat, other thermodynamic and elastic properties, which would be in good agreement with the various experimental observations and (ii) to carry out molecular dynamics simulations using the parameters obtained from the lattice dynamics calculations to elucidate the microscopic picture of the cation diffusion with increasing temperature. This would throw light on the mechanism of fast ion diffusion and the scenario in the crystal lattice just beyond the transition point. Experimental data on the diffusion coefficient,[30] specific heat, mean squared displacements, elastic properties,[27] and phonon frequencies[31,32] in Li_2O are available.

This paper has been divided into several sections. Section II presents the details of the comprehensive lattice dynamics calculations. Section III deals with the details of the molecular dynamics simulation. Section IV summarizes and discusses the numerous results obtained using both the techniques. Finally, the various inferences concluded from the earlier studies have been put forth in Sec. V.

II. LATTICE DYNAMICS CALCULATIONS

Our calculations have been carried out in the quasiharmonic[33] approximation using the interatomic potentials consisting of Coulomb and short-range Born-Mayer type interaction terms

$$V(r_{ij}) = \frac{e^2}{4\pi\mathcal{E}_0}\frac{Z(k)Z(k')}{r_{ij}^2} + a\exp\left[\frac{-br_{ij}}{R(k)+R(k')}\right], \quad (1)$$

where r_{ij} is the separation between the atoms i and j of type k and k', respectively. R (k) and Z (k) are the effective radius and charge of the kth atom, a and b are the empirical parameters optimized from several previous calculations.[34] Oxygen atoms have been modeled using a shell model,[33] where a massless shell of charge Y (k) is linked to the atomic core by harmonic force constant K (k). Lattice constant, zone center phonon frequencies and elastic constants have been fitted to experimental values. The final set of optimized parameters used in the calculation is given in Table I. The calculations have been carried out using the current version of the software DISPR[35] developed in Trombay. The interatomic potential enables the calculation of the phonon frequencies in the entire Brillouin zone. Based on the crystal symmetry, group theoretical analysis provides a classification of the frequencies at zone center and the symmetry directions, in the following representations:

$$\Gamma\text{: } 2T_{1u} + T_{2g} \ (T_{1u} \text{ and } T_{2g} \text{ are triply degenerate}),$$

$$(00\zeta)\text{: } 2\Delta_1 + \Delta_2 + 3\Delta_3,$$

$$(\zeta\zeta 0)\text{: } 3\Sigma_1 + 2\Sigma_2 + \Sigma_3 + 3\Sigma_4,$$

$$(\zeta\zeta\zeta)\text{: } 3\Lambda_1 + 3\Lambda_3.$$

(Λ_3 and Δ_3 modes are doubly degenerate.)

Based on the crystal symmetry, Li_2O is expected to have one infrared active mode (T_{1u}) and one Raman active optical mode (T_{2g}). These classifications of the phonon modes into different irreducible representations enable direct comparison with single crystal Raman, infrared and neutron data.

Phonon density of states is an integrated average over all phonon modes in the complete Brillouin zone. It is defined by the equation

$$g(\omega) = c\int_{BZ}\sum_j \delta[\omega - \omega_j(\boldsymbol{q})]d\boldsymbol{q}, \quad (2)$$

where c is a normalization constant such that $\int g(\omega)d\omega = 1$, $\boldsymbol{q}$ is the reduced wave vector in the Brillouin zone, ω_j is the frequency of the jth phonon mode; Phonon density of states has been calculated by effectively integrating over a $8\times8\times8$ mesh of wave vectors in the cubic reciprocal space unit cell while taking advantage of the symmetry of the Brillouin zone. The contribution from individual atom species can be obtained as partial density of states, which is given as

TABLE I. Model parameters ($a = 1822$ eV, $b = 12.364$).[34]

Atom type (k)	R (k) (nm)	Z (k)	Y (k)	K (k) (eV/nm^{-2})
Lithium	0.129	0.75	⋯	⋯
Oxygen	0.175	−1.5	−2	6500

$$g_k(\omega) = c\int\sum_j |\xi(\boldsymbol{q}j,k)|^2\delta[\omega - \omega_j(\boldsymbol{q})]d\boldsymbol{q}, \quad (3)$$

where ξ $(\boldsymbol{q}j,k)$ is the polarization vector of the phonon ω_j $(\boldsymbol{q}j)$. The calculated density of states can be used to evaluate the various thermodynamic properties of the solid including specific heat at constant volume, $C_V(T)$. To compare with experimental data, we need to calculate $C_P(T)$, which is given as

$$C_P(T) = C_V(T) + \alpha_v(T)^2BVT, \quad (4)$$

$$\text{where bulk modulus, } B = -V\left(\frac{dP}{dV}\right). \quad (5)$$

The volume coefficient of thermal expansion is given as

$$\alpha_v(T) = \frac{1}{BV}\sum_{i=\boldsymbol{q}j}\Gamma_i C_{v_i}(T). \quad (6)$$

Γ_i is the Grueneisen parameter for the jth phonon mode at wave vector $\mathbf{q}$ and is given by

$$\text{Gruneisen parameter, } \Gamma_i = -\frac{\partial \ln \omega_i}{\partial \ln V}. \quad (7)$$

In the present work, we have calculated the phonon frequencies, the elastic constants, the specific heat, and the equation of state. These results have been compared with the available experimental data in Sec. IV.

III. MOLECULAR DYNAMICS SIMULATION

Molecular dynamics is a powerful method for exploring the structure and dynamics of solids, liquids, and gases. Explicit computer simulation of the structure and dynamics using this technique allows a microscopic insight into the behavior of materials to understand the macroscopic phenomenon like diffusion of lithium ions and their contribution to the fast ion transition in this case. An interatomic potential, which treats Li and O as rigid units may be sufficient to study properties like diffusion. The optimized parameters obtained from lattice dynamics studies have been used for these simulations. In our study, we have taken a macro cell of 768 rigid atoms with periodic boundary conditions to study the response of the system when set free to evolve from a configuration disturbed from the equilibrium situation. The lattice parameters and atomic trajectories can thus be obtained as a function of temperature and external pressure. Calculations in this work have been done using the software developed at Trombay.[36] The simulations have been done at various temperatures up to and beyond the fast ion

TABLE II. Comparison between calculated and experimental lattice[1] parameters and elastic constants[27] at ambient conditions. The numbers in the parenthesis are the errors in the last significant digit.

Physical Quantity	Experiment	Calculated
Lattice parameter (nm)	0.460 (1)	0.461
Bulk modulus	81.7(62)	103
C_{11} (GPa)	202.0 (55)	213
C_{44} (GPa)	58.7 (8)	52
C_{12} (GPa)	21.5 (66)	56
C_{11}-C_{12} (GPa)	180.5 (86)	157
Anisotropy factor $(2C_{44}/(C_{11}—C_{12}))$	0.65 (5)	0.66

transition. The diffusion coefficient, mean square displacement of lithium ion, and the pair correlation function were calculated to understand the local environment in the normal as well as the superionic phase and to understand the changes taking place upon transition.

The pair correlation function of a crystal consisting of various atoms at a given r is dependent on

$$g_{k'k}(r) \propto \frac{1}{4\pi r^2} \sum_{i,j}^{i \neq j} \delta\{r - r_{ij}(kk')\}, \tag{8}$$

where r_{ij} (kk') is the separation between the positions of ith and jth constituent atoms while k and k' refer to the different kinds of atoms. Molecular dynamics simulations have been carried out at various temperatures starting from 300 to 1500 K at zero pressure and 5 GPa. The diffusion of lithium and oxygen ions have been monitored. The effect of static pressure on the diffusion of constituent ions has also been investigated. The movement of certain lithium ions over a time of 10 ps was monitored with a time step of 1 fs to understand the diffusion dynamics, taking place in the lithium sublattice.

IV. RESULTS AND DISCUSSION

The calculated values of the lattice parameter, bulk modulus, and elastic constants compare well with the experimentally obtained data as presented in Table II. From the phonon dispersion relation along [110], we can obtain the value of $C_{11}—C_{12}$ for cubic systems, which is in good agreement with its corresponding experimental value. Since C_{12} is derived indirectly using the values of C_{11} and $(C_{11}—C_{12})$, it appears to be overestimated, as compared to the experimen-

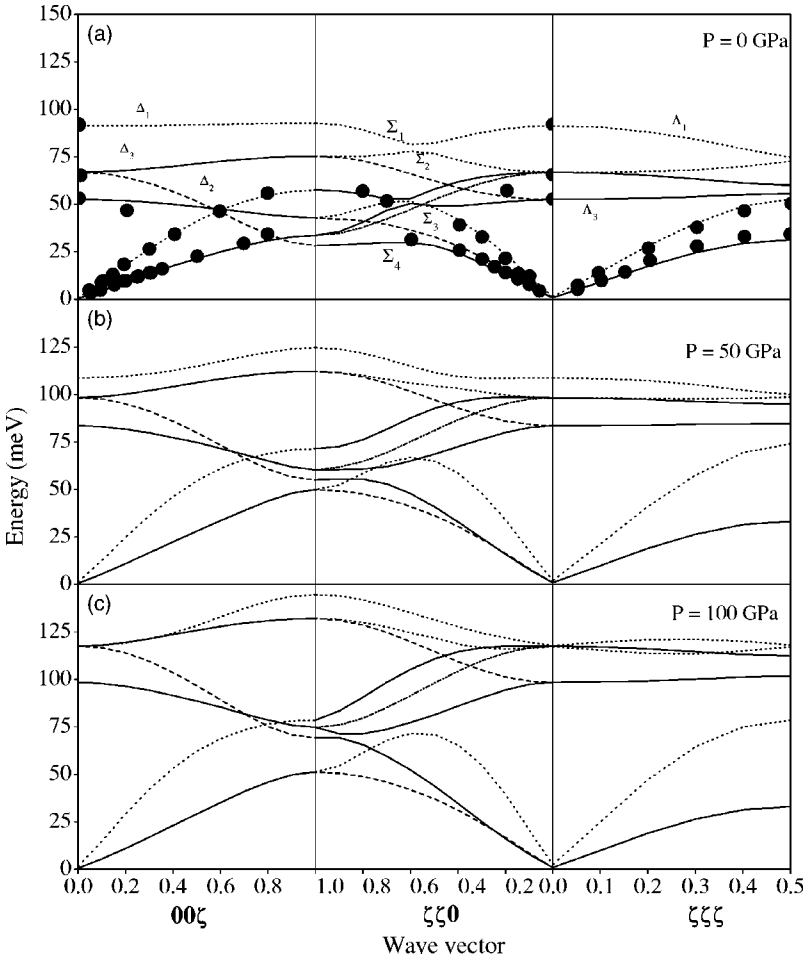

FIG. 1. Phonon dispersion relation in Li_2O; (a) $P=0$ GPa, (b) $P=50$ GPa, and (c) $P=100$ GPa. Solid symbols are the experimental[31] points from neutron scattering.

TABLE III. Comparison between experimentally obtained light scattering data[32] and the calculated values.

Mode	Experiment	Calculated
T_{1u} (TO) (cm^{-1})	737	737
T_{1u} (LO) (cm^{-1})	425	423
T_{2g} (cm^{-1})	523	539

tal results.[27] The calculated phonon dispersion relation in lithium oxide is given in Fig. 1 at three different pressures. The calculated zone center mode frequencies have been compared with light scattering data in Table III. The values of Γ_i for the zone center optic modes have been calculated; $\Gamma_{T_{1u}}=0.66$ [for the longitudinal optical (LO) branch]; $\Gamma_{T_{1u}}=1.68$ [for the transverse optical (TO) branch]; $\Gamma_{T_{2g}}=1.47$ for the Raman mode. Figure 1 and Table III show that the agreement of the calculations with the single crystal neutron,[31] Raman, and infrared data[32] is excellent. The calculated ratio between the static-dielectric constant $\varepsilon(0)$ to its high frequency limit $\varepsilon(\infty)$, $\varepsilon(0)/\varepsilon(\infty)=3$, is in good agreement with experiment.[32]

With the increase in pressure, our calculations do not indicate any softening of the phonon modes. In general, all the frequencies have hardened with pressure; especially phonons in the energy interval between 50 and 75 meV at $P=50$ GPa show a shift of about 25 meV towards the higher end, while the top most branch shifts by only about 15 meV. With further increase in pressure to 100 GPa, the above frequencies harden further by 15 meV.

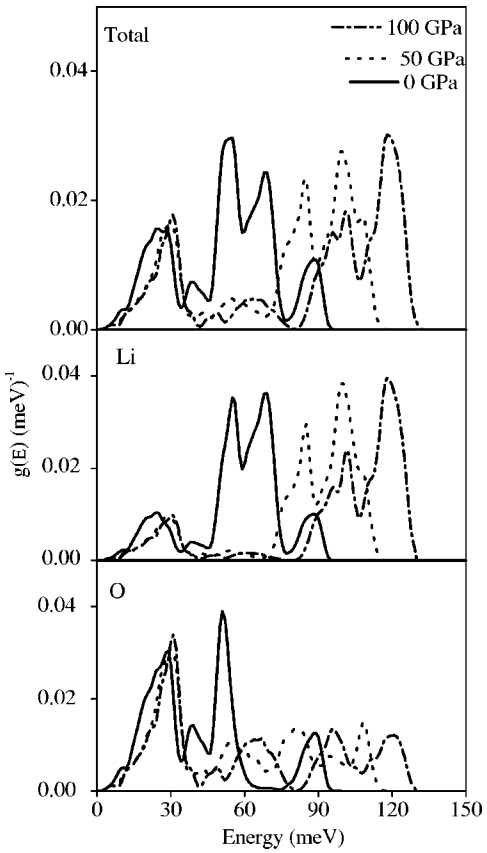

FIG. 2. Phonon density of states at $P=0$ GPa, $P=50$ GPa, and $P=100$ GPa along with the partial density of states for lithium and oxygen as calculated by quasiharmonic lattice dynamics calculations.

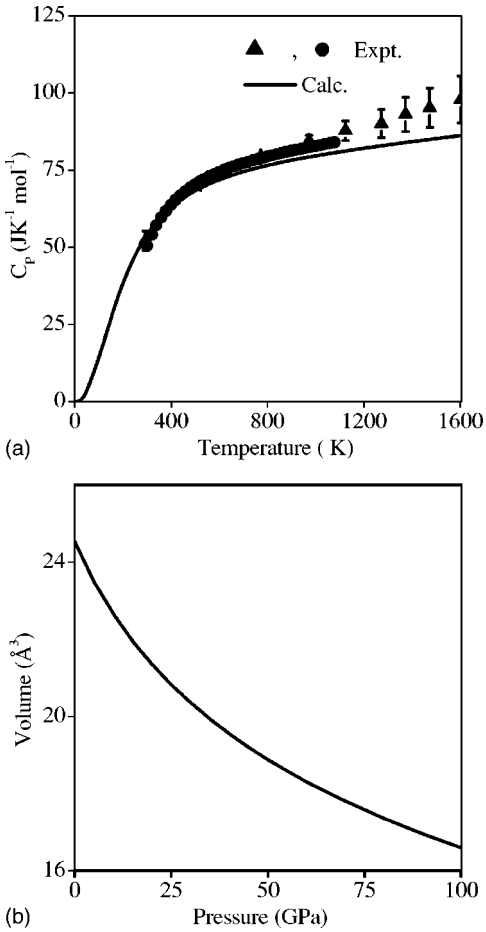

FIG. 3. (a) Specific heat at constant pressure compared with experimental[27,29] data (circles[29] and triangles[27]). (b) The equation of state for Li_2O.

These observations are further substantiated from the total density of states, and the partial densities for Li and O atoms in Fig. 2. The energy span at $P=0$ GPa is between 0 and 90 meV, at $P=50$ GPa, it is up to 120 meV, while at $P=100$ GPa it spans up to 135 meV. As can be seen from the figure, the peak around 50 meV at $P=0$ GPa has shifted to higher energy with pressure increase, while the peak around 20 meV is more or less undisturbed. From the partial densities, we can conclude that the oxygen contribution is much greater on the lower energy end, which remains unperturbed by pressure changes, suggesting its greater stability compared to lithium. At $P=0$ GPa, lithium ion's contributions lie mainly in the interval 45–75 meV, likewise oxygen atom's contribution lies mainly in the interval 0 and 60 meV. There is a contribution from both atoms at 90 meV. At $P=50$ GPa, lithium atoms contribute between 75 and 120 meV while oxygen atoms contribute up to 120 meV. At 100 GPa, lithium contributes mainly between 85 and 135 meV, while oxygen contributes until 135 meV. At all the three pressures, the lowest peak for both the atoms are practically indistinguishable.

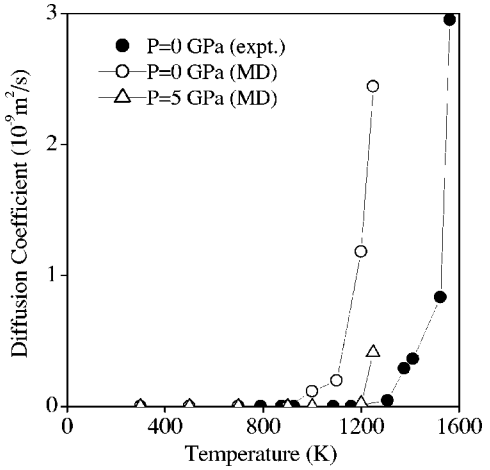

FIG. 4. Lithium atom's diffusion coefficient, D and its variation with temperature and pressure obtained from molecular dynamics (MD) simulations. Solid circles are the experimental results[30] at ambient pressure.

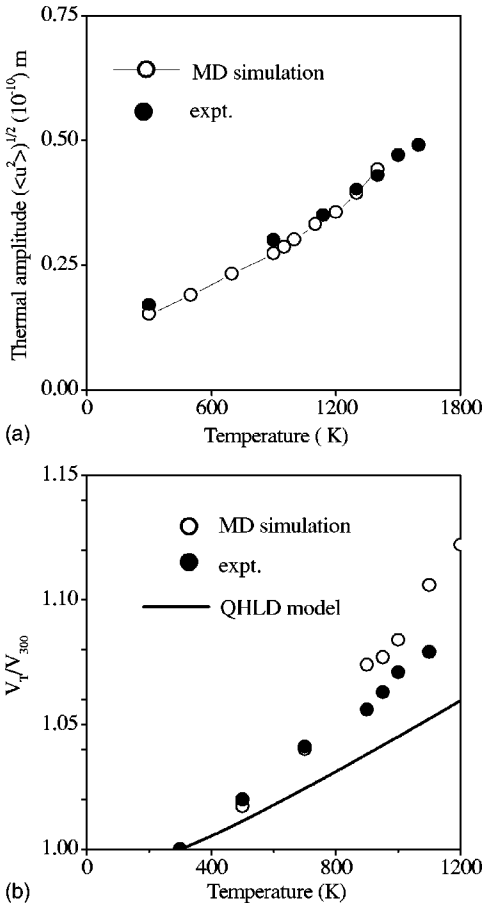

FIG. 5. (a) Calculated (MD simulations) thermal amplitude of lithium $\langle u^2\rangle^{1/2}$ as a function of temperature (open circles) at ambient pressure and comparison with experiment (solid circles).[1] (b) Variation of lattice volume with temperature at ambient pressure, compared with experimental[27] (solid circles) results. Open circles, as derived from molecular dynamics simulations, denote calculated values. Full line gives the thermal expansion derived from quasiharmonic lattice dynamics calculations.

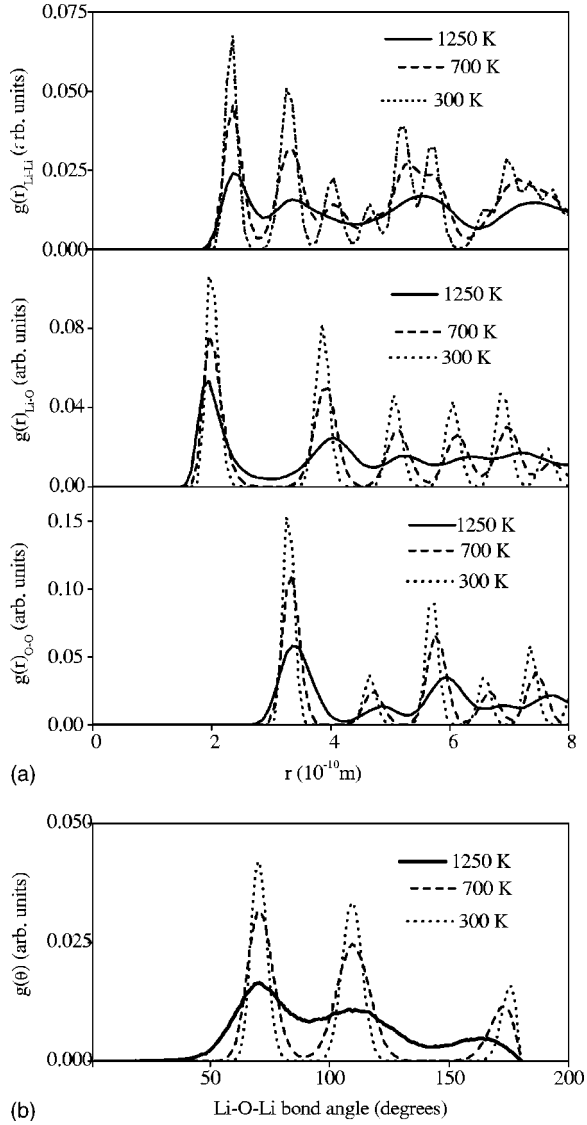

FIG. 6. (a) Pair correlation functions of Li—Li, Li—O, and O—O and (b) angle correlation function of Li—O—Li bond angle in Li_2O at different temperatures and ambient pressure as obtained from MD simulations.

The calculated specific heat, $C_P(T)$, has been compared with the available experimental data[27,29] in Fig. 3(a). The comparison is very good up to about 1100 K beyond which the fast ion behavior sets in and the slope of the experimental data are much greater compared to calculations. This is expected owing to the quasiharmonic approximation in lattice dynamics calculations.

The equation of state, i.e., the variation of the volume of the primitive cell with pressure, is given in Fig. 3(b), however, experimental data for the same is unavailable for comparison. There is a smooth decrease in volume with increase in pressure.

The diffusion coefficient of lithium ion has been compared with experimental[30] data in Fig. 4. The experimental[30] transition temperature of the normal to fast ion phase is about 1200 K at zero pressure whereas the calculated value lies at about 1000 K, which is in good agreement. The ap-

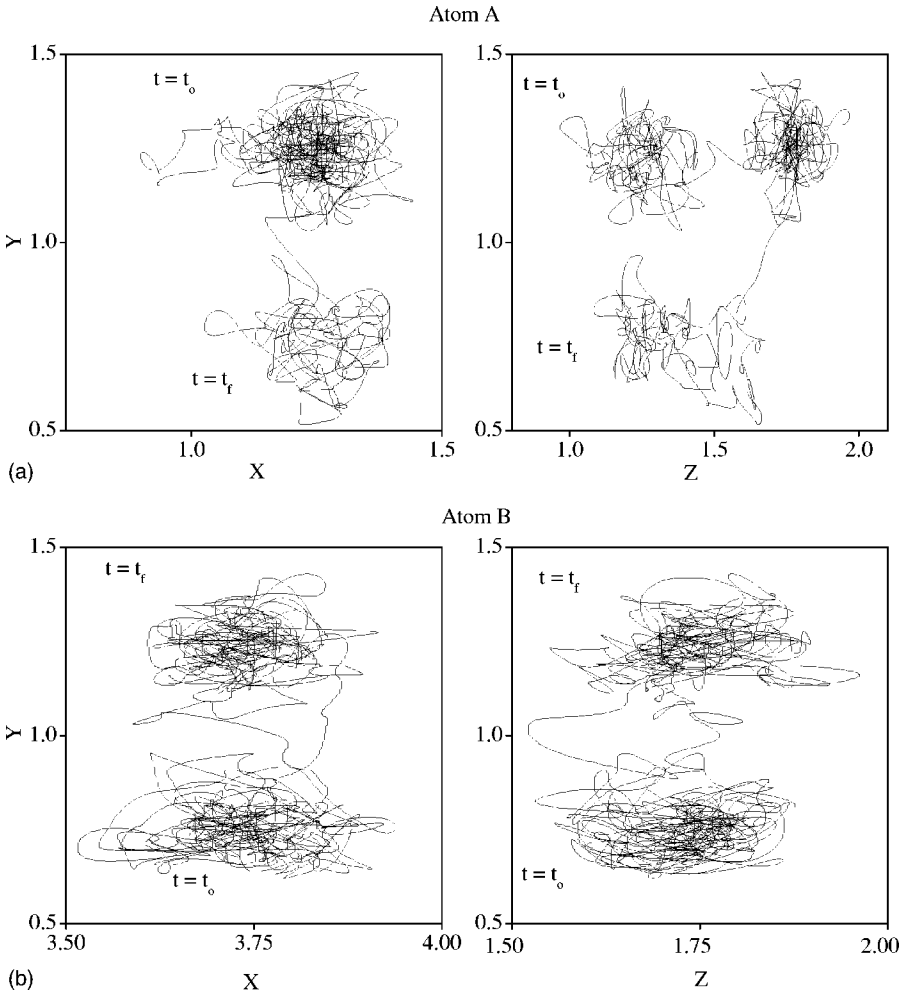

FIG. 7. Snapshots of the movement of given lithium atoms (a) atom A and (b) atom B in a duration of 10 ps in the *XY* and *YZ* planes as obtained from molecular dynamics simulations at 1250 K and ambient pressure. The values in the *x* axis are actually multiples of the lattice parameter at 1250 K. Lithium atoms preferentially occupy only the tetrahedral sites.

plication of a static pressure of 5 GPa increases T_c only marginally by 200 K to about 1200 K.

The thermal amplitude of lithium atom is compared with experimental results[1] in Fig. 5(a), which are in very good agreement. The change in the slope of the plot at the superionic transistion, which is seen in the experiment, is brought out clearly. The variation of the volume of the unit cell with temperature, as obtained from molecular dynamics simulations is plotted in Fig. 5(b), which shows a good agreement with experiment.[27] The implicit thermal expansion calculated from quasiharmonic lattice dynamics arising from the volume dependence of phonon frequencies is also plotted, which accounts for only a part of the observed thermal expansion.

The disturbances in the crystal structure accompanying the superionic transition are limited to the lithium sub lattice. This conclusion is further strengthened by the pair correlation functions of Li—Li, Li—O, and O—O in Fig. 6(a). But it is also noteworthy to mention that the disturbances in the lithium sublattice occur gradually as seen from the broadening in the pair correlation functions of Li—Li with increasing temperature. On similar lines, we can understand the angle distribution of Li—O—Li bond in Fig. 6(b), which again shows no drastic changes near the fast ion transition. This reiterates the notion that the disturbances occurring in the lattice are highly localized and the local environment is only moderately disturbed. The oxygen sub lattice remains unperturbed as seen from the plots in Fig. 6.

The position—time plots of certain Li atoms, for a time duration of 10 ps at 1250 K in *XY* and *YZ* planes are given in Fig. 7. The Li atom A at an initial position (the positions are actually multiples of the lattice parameter) of (1.25,1.25,1.25) moves to a second position (1.25,1.25,1.75) with a jump time of approximately 0.065 ps, residence time being more than 3.3 ps at the initial position. It then moves to the third position of (1.25,0.75,1.25). The residence time at the second position is 3.9 ps. Before moving to the third position, it undergoes some transit zigzag motion in the octahedral region surrounding the coordinate (1.25,1.65,1.5). On the other hand atom B starts at an initial coordinate of (3.75,0.75,1.75) and then moves to the second position (3.75,1.25,1.75) in the time duration for which these atoms were tracked. These results indicate that the lithium atoms jump from one tetrahedral position to another, passing the octahedral interstitial regions during transit; at any given instant the probability of an atom sitting in the octahedral position is rather small. Similar results have been reported for CuI,[14,15] where ionic density distribution shows no or very little occupation of the octahedral sites with increase in temperature. Average potential energy curves obtained for CuI[14] depict that energy is a minimum at the tetrahedral sites and rises rapidly as the octahedral site is approached. The lithium

atoms essentially move from one tetrahedral position to another randomly, yet maintaining the local order and structure to a great degree.

V. CONCLUSIONS

A shell model has been successfully used to study the phonon properties of lithium oxide. The interatomic potential is able to reproduce the elastic constants, bulk modulus, equilibrium lattice constant, and phonon frequencies, which are in good agreement with the reported data.[1,27,29,31,32] The calculated phonon dispersion relation is in very good agreement with the reported neutron and light scattering data.[31,32] There appears no phonon softening even up to high pressures of 100 GPa. Partial densities of state of lithium and oxygen atoms show that they contribute almost in the whole energy span up to 100 meV. There is a greater contribution of lithium in the higher energy side as compared to oxygen, which contributes more on the lower end. This may be explained with regards to their size and mass. The calculated specific heat is in good agreement up to about 1100 K but shows a slower rise as compared to the experimental data when the superionic behavior sets in. Small deviations between the calculation and the experiment begins to occur even at lower temperature which could be due to some defect generation in the lattice prior to the superionic phase.

The diffusion coefficient calculated for lithium ion shows a transition to fast ion phase at around 1000 K whereas in experiment, it is seen to occur around 1200 K. At the transition temperature, lithium atom's diffusion coefficient is comparable to that of a liquid and is in the order of 10^{-9} m^2/s. Application of static pressure of 5 GPa only brings about a marginal change in the transition temperature. The pair correlation functions for Li—Li, Li—O, and O—O and the angle distribution for Li—O—Li bring out the following inferences. The pair correlations for Li—Li just show a gradual broadening with increase in temperature from 300 to 1250 K. The distortions in the lattice due to fast ion diffusion are highly localized, and the local environment remains unchanged to a great extent. These results indicate to a jump diffusion model in which the lithium ions move from one tetrahedral site to another tetrahedral site via octahedral interstitial sites. But nonetheless, they do not occupy any of these octahedral sites. The jump time of the lithium atoms at temperatures above the transition is very small compared to their residence time at any given symmetry position. As a result, the lattice seems more or less undisturbed. Though there is a considerable movement of lithium atoms, we could not discern any rule governing their movements from one tetrahedral region to another. The interatomic potential formulated for lithium oxide may be transferred to other similar fluorite and antifluorite oxides like Na_2O, K_2O, UO_2, ThO_2, etc. with suitable modifications to study their vibrational and thermodynamic properties.

[1] T. W. D. Farley, W. Hayes, S. Hull, M. T. Hutchings, and M. Vrtis, J. Phys.: Condens. Matter **3**, 4761 (1991).
[2] R. W. G. Wyckoff, *Crystal Structures*, 2nd ed. (Wiley, New York, 1963).
[3] D. A. Keen, J. Phys.: Condens. Matter **14**, R819 (2002).
[4] G. L. Kalucinki, J. Nucl. Mater. **141**, 3 (1986).
[5] R. Shah, A. De Vita, H. Heine, and M. C. Payne, Phys. Rev. B **53**, 8257 (1996).
[6] J. G. Rodeja, Modell. Simul. Mater. Sci. Eng. **9**, 81 (2001).
[7] R. M. Fracchia, G. D. Barrera, N. Allan, T. H. K. Barron, and W. C. Mackrodt, J. Phys. Chem. Solids **59**, 435 (1998).
[8] A. De Vita, I. Manasidis, M. J. Gilan, and J. S. Lin, Europhys. Lett. **19**, 605 (1992).
[9] J. H. Strange, S. M. Rageb, A. V. Chadwick, and K. W. Flack, J. Chem. Soc., Faraday Trans. **86**, 1239 (1990).
[10] S. Albrecht, G. Onida, and L. Reining, Phys. Rev. B **55**, 10 278 (1997).
[11] P. W. M. Jacobs and M. L. Vernon, J. Chem. Soc., Faraday Trans. **86**, 1233 (1990).
[12] A. Shukla, M. Dolg, and P. Fulde, J. Chem. Phys. **108**, 8521 (1998).
[13] R. Dovesi, C. Roetti, C. Freyria-Fava, and H. Prencipe, Chem. Phys. **156**, 11 (1991).
[14] J. X. M. Zheng-Johannson and R. L. McGreevy, Solid State Ionics **83**, 35 (1996).
[15] K. Ihata and H. Okazaki, J. Phys.: Condens. Matter **9**, 1477 (1997).
[16] D. A. Keen and S. Hull, J. Phys.: Condens. Matter **7**, 5793 (1995).
[17] M. Hofmann, S. Hull, G. J. McIntyre, and C. C. Wilson, J. Phys.: Condens. Matter **9**, 845 (1997).
[18] R. B. Roberts and G. K. White, J. Phys. C **19**, 7167 (1986).
[19] M. H. Dickens, W. Hayes, M. T. Hutchings, and W. G. Klepmann, J. Phys. C **12**, 17 (1979).
[20] W. G. Kleppmann, J. Phys. C **11**, L91 (1978).
[21] M. H. Dickens, W. Hayes, P. Schnabel, M. T. Hutchings, R. E. Lechner, and B. Renker, J. Phys. C **16**, L1 (1983).
[22] M. M. Elcombe and A. W. Pryor, J. Phys. C **3**, 492 (1970).
[23] C. R. A. Catlow, J. D. Comins, F. A. Germano, R. T. Harley, and W. Hayes, J. Phys. C **11**, 3197 (1978).
[24] M. T. Hutchings, K. Clausen, M. H. Dickens, W. Hayes, J. K. Kjems, P. G. Schnabel, and C. Smith, J. Phys. C **12**, 3941 (1984).
[25] M. Wilkening, S. Indris, and P. Heitjans, Phys. Chem. Chem. Phys. **5**, 2225 (2003).
[26] A. De Vita, M. J. Gilan, J. S. Lin, M. C. Payne, I. Stich, and L. J. Clarke, Phys. Rev. Lett. **68**, 3319 (1992).
[27] S. Hull, T. W. D. Farley, W. Hayes, and M. T. Hutchings, J. Nucl. Mater. **160**, 125 (1988).
[28] T. Kurusawa, T. Takahashi, K. Noda, H. Takeshita, S. Nasu, and H. Watanbe, J. Nucl. Mater. **107**, 334 (1982).
[29] T. Tanifugi, K. Shiozawa, and S. Nasu, J. Nucl. Mater. **78**, 422 (1978).
[30] Y. Oishi, Y. Kamwei, and M. Akuyama, J. Nucl. Mater. **87**, 341 (1979).
[31] T. W. D. Farley, W. Hayes, S. Hull, and R. Ward, Solid State

Ionics **28–30**, 189 (1988).
[32] T. Osaka and I. Shindo, Solid State Commun. **51**, 421 (1984).
[33] G. Venkataraman, L. Feldkamp, and V. C. Sahni, *Dynamics of Perfect Crystals* (MIT Press, Cambridge, 1975); P. Bruesh, *Phonons: Theory and Experiments* (Springer-Verlag, Berlin, 1986).
[34] K. R. Rao, S. L. Chaplot, N. Choudhury, S. Ghose, J. M. Hastings, L. M. Corliss, and D. L. Price, Phys. Chem. Miner. **16**, 83 (1988); S. L. Chaplot, N. Choudhury, S. Ghose, M. N. Rao, R. Mittal, and P. Goel, Eur. J. Mineral. **14**, 291 (2002).
[35] S. L. Chaplot, Report BARC-972, 1978; (unpublished).
[36] S. L. Chaplot and K. R. Rao, Phys. Rev. B **35**, 9771 (1987); S. L. Chaplot, *ibid.* **42**, 2149 (1990); S. L. Chaplot and N. Choudhury, Am. Mineral. **86**, 752 (2001).